Kakoee, A.; Bakhshan, Y.; Barbier, ARS.; Bares-Moreno, P.; Guardiola, C. (2020). Modeling combustion timing in an RCCI engine bymeans of a control oriented model. Control Engineering Practice. 97:1-15. https://doi.org/10.1016/j.conengprac.2020.104321

Modeling combustion timing in an RCCI engine by means of a control oriented model

A. Kakoee[1], Y. Bakhshan[*1], A. Barbier[2], P .Bares[2], C. Guardiola[2]

1- Department of Mechanical Engineering, University of Hormozgan, Bandar Abbas, Iran

2 - *CMT-Motores Térmicos, Universitat Politècnica de València, Camino de Vera s/n, E-46022, Valencia, Spain*

Abstract

Reactivity controlled compression ignition (RCCI) engines as one of low temperature auto ignition combustion strategies have shown a good performance to reduce NO_x and soot emission while increasing engine thermal efficiency. Combustion control of these types of engines is relatively complex because of their ignition type which makes it difficult to have a direct control on the start of the combustion. In this research, combustion phase of an RCCI engine was modeled with using a control-oriented method. The combustion properties such as start of the combustion, crank angle degree where 50 percent of the fuel is burnt(CA50) and the burn duration were modeled in this research. A modified knock integral model was used for start of combustion estimation. Using the effect of spontaneous front speed, burn duration was modeled where a mathematical model is developed; and Wiebe function is used to model CA50. Indicated mean effective pressure(IMEP) also estimated in this modeling. To validate the developed models, five experimental data sets from a heavy-duty RCCI engine were used. The results show the maximum mean errors of 1.7, 1.9 and 2.3 crank angle degree (CAD) for start of combustion, burn duration(BD) and the CA50, respectively and this quantity is 0.5 bar for IMEP in steady state condition. The transient condition of the engine operation was also investigated. The results and trends are promising in all characteristics of the combustion process especially in the modeling of the indicated mean effective pressure where the majority of the data have errors less than 1.5 bar.

Keywords: RCCI engine, control oriented method, Modified knock integral model, CA50, burn duration, start of combustion, IMEP

RCCI	Reactivity control compression ignition	n	constant of Arrhenius equation
SOC	Start of combustion	Ea	energy of activation
CAD	Crank angle degree	C1	constant in Ea equation
COM	control oriented method	C2	constant in Ea equation
CA50	crank angle degree where 50 percent of fuel burned	CN_{mix}	Cetane number of fuel mixture
BD	Burn duration	CN_{pfi}	Cetane number of Pfi
HCCI	Homogeneous charge compression ignition	CN_{di}	Cetane number of Direct injection
PCCI	premixed charge compression ignition	GF	Gasoline fraction
LTC	Low temperature combustion	φ_{DI}	global equivalence ratio of diesel
LRF	low reactivity fuel	φ_{pfi}	global equivalence ratio of port fuel injection
HRF	High reactivity fuel	a_1	Constant in A equation multiply to relation of it
CI	compression ignition	a_2	Constant in A equation and is power of φ_{DI}

[*] Corresponding author: Tel/Fax: +98 7636671088
Email: Bakhshan@hormozgan.ac.ir (Y.Bakhshan)

SI	spark ignition
EGR	exhaust gas recirculation
PID	proportional integral derivative
MKIM	modified knock integral model
Pint	Intake pressure
$[CO_2]_{int}$	concentration of CO2 in intake air mixture
$[CO_2]_{atm}$	concentration of CO2 in atmosphere
$[CO_2]_{exh}$	concentration of CO2 in exhaust gas
PXIe-8135	real-time National Instruments controller
FPGA	Field Programmable Gate Array
PXIe-6358	16 analog channels acquisition card
IVC	Inlet valve close
EOC	end of combustion
CA90	the angle where 90 percent of fuel mixture burns
T_{IVC}	Temperature at IVC
P_{IVC}	Pressure at IVC
V_{IVC}	Volume at IVC
m_{cyc}	Amount of mass trapped in the cylinder
η_v	volumetric efficiency
V_{dis}	displacement volume
P(θ)	pressure at each CAD
T(θ)	temperature at each CAD
V(θ)	Volume at each CAD
k	Constant of polytropic equation for compression
θ_{SOC}	SOC crank angle in degree
θ_{IVC}	IVC crank angle in degree
Pfi	Port fuel injection
Di	Direct injection
A	Constant related to concentration of fuel
N	engine speed in rpm
b	constant related to fuel reactivity
$[O_2]_{int}$	Concentration of inlet oxygen
$[O_2]_{atm}$	Atmosphere oxygen concentration
$[O_2]_{exh}$	concentration of exhaust oxygen
T_{evo}	Exhaust valve open temperature
T_{eoc}	End of combustion temperature
T_{rg}	Residual gas temperature
$IMEP$	Indicated mean effective pressure
$T_{ivc,mix}$	Temperature of in-cylinder mixture at IVC
T_{rg}	Residual gas temperature
a_3	Constant in A equation and is power of φ_{pfi}
a_4	Constant in A equation and is power of $[O_2]_{int}$
SOI	Start of ignition
τ	Delay time function from SOI to SOC
t	Delay time
$\vec{V}$	Vector of spontaneous front speed
S_{ig}	Spontaneous front speed
Tc	corrected temperature for BD modeling
Pc	corrected pressure for BD modeling
T_{SOC}	Temperature at SOC
p_{SOC}	Pressure at SOC
ΔT	Temperature rise related to complete combustion
$Q_{\mathrm{LHV,di}}$	Low heat value of diesel
$Q_{\mathrm{LHV,pfi}}$	Low heat value for port fuel injection fuel
$FAR_{\mathrm{st,di}}$	stoichiometric fuel air ratio of direct injected fuel
$FAR_{\mathrm{st,pfi}}$	stoichiometric fuel air ratio of port fuel injection
C_v	heat capacity of a gas held at constant volume
e_1	constant in temperature correction
e_2	constant in pressure correction
d_0, d_1, d_2	constants in e1 equation
e_0, e_1, e_2	constants in e2 equation
K_1	constant in BD estimation
ζ	constant in BD estimation and is power of Sig
x_b	fraction of fuel burned in each CAD
n_e	Polytropic expansion coefficient
a and m	constants in Wiebe function
AHRR	Apparent heat release rate
θ	Crank angle in degree
LTHR	low temperature heat release
HTHR	High temperature heat release
CHR	Cumulative heat release
LHV	Lower heating value
P_{evo}	Exhaust valve open pressure
P_{eoc}	End of combustion pressure
θ_d	Burn duration in CAD
x_d	Dilution factor
P_{exh}	Exhaust pressure
r_c	Compression ratio
m_{rg}	Residual gas mass

1. Introduction

Homogeneous charge compression ignition (HCCI), premixed charge compression ignition (PCCI) and reactivity controlled compression ignition(RCCI) are three concepts of low temperature combustion(LTC) used to reduce engine pollutants such as NO_x and soot emissions coming from compression ignition (CI) engine exhaust. Among these three types of LTC, RCCI engines have better performance for reducing NO_x and soot emissions while increasing thermal efficiency [1]. The main goal of the RCCI combustion strategy is to control emissions specially NOx and soot by controlling the in-cylinder reactions in the way of low temperature and lean combustion. There are two type of fuels in an RCCI engine with low and high reactivity properties. The low reactivity fuel is usually injected through the intake valve to the combustion chamber with air, this fuel helps to reduce temperature of combustion with consuming part of in-cylinder produced energy beside keeps engine efficiency in high level, low reactivity fuel also helps to have more complete combustion in combustion chamber and as a result lower unburned hydrocarbons. [2-3] Moreover, controlling combustion of RCCI is easier than those of HCCI and PCCI [4-6]. In contrast to ordinary compression ignition(CI) and spark ignition(SI) engines, having direct control on RCCI engines is difficult because of the type of start of combustion (SOC) [7]. Nevertheless, investigating of heat release rate and combustion control of this type of engine have shown better results in according to two-fuel engines [8, 9]. This type of combustion is sensitive to intake conditions such as temperature, pressure and amount of exhaust gas recirculation (EGR) in a complete cycle of combustion. [10].

Precise control of combustion phenomenon in internal combustion engines can have valuable results on the performance and thermal efficiency of engine. Two main methods have been proposed by literature to control the combustion. First, the proportional integral derivative(PID) method which is used by Olsson et al. in [11]. This method is also used by Hanson and Reitz in [12] and by Arora and Shahbakhti in [13]. Control Oriented Method (COM) is another strategy to model combustion of the engine. Since COM provides a faster solution and can be used in a real time control system, it has been very attractive to researchers [14-17]. Bekdemir et al. [15] used a multi-zone approach to model combustion in a natural gas-diesel RCCI heavy duty engine to investigate auto-ignition process and to make a prediction of pressure trace. Khodadadi and Shahbakhti used this method on a research case in 2016. They modeled SOC, BD and CA50 during their investigation using numerical data cases [16]. Recently, in 2017, Nithin et al. [17]. have investigated the combustion phase in a transient and steady state condition with applying COM. They used a modified knock integral model (MKIM) based on the research done by Livengood and Wu in [28] to model SOC and the Wiebe function for CA50 [17]. Similar modeling has been done by Shahbakhti in 2016 [18] and Khodadadi Sadabadi, K. et al. in 2010 [20]. Recently in 2019, Sui W and Pulpeiro et al. used two different close loop and open loop controller to estimate combustion characteristic of an RCCI six cylinder engine [21]. Genetic Algorithm (GA) also was used to predict start of combustion in a HCCI engine, M.Taghavi et al., in their study Artificial Neural Network (ANN) was used as a low computational time consuming method to predict SOC.[40].

There are also some researches on modeling combustion process in HCCI engines such as Arrhenius-like model by Shaver in 2004 [22] and Mayhew's work in 2009 [23]. In contrast to MKIM, combustion modeling in this field of research is related to the fuel and oxygen concentration. Also, some researchers tried to eliminate oxygen and fuel concentration effects [24, 25].

Delay time function which represent time before start of combustion plays an important role in control oriented method. In previous researches different parameters were used in time function. In 2005 X.He et

al used a time function with different parameters which are equivalence ratio, temperature, pressure and intake oxygen mole fraction in their delay time function, in their research it has been tried to observe effects of temperature and pressure beside composition of mixture on an HCCI engine operational conditions [25], this function also used by S. Scott Goldsborough in 2009 in different applications, rapid compression machine and shock tube. [27]. In recent works for RCCI modeling equivalence ratio (ER) of different fuels, temperature, pressure and energy of activation were considered in time equation by Nithin et al., focuses in their works are on predicting combustion characteristics in variation of start of injection and premixed ratio [17]. Khodadadi Sadabadi et al. in 2016 used various parameters in their physical concepts, such as SOI and EGR percentages, they have also investigations on transient operational conditions. [20] and Akshat Raut et al in 2018 [38]. Sui W et al used a delay time which is a function of global equivalence ratio of each fuel, temperature, pressure and EGR [21]. In current study a delay time function is a function of equivalence ratio of each fuel, inlet oxygen percentage, temperature, pressure and Cetane number of fuel mixture with focusing on calibration CA50 and IMEP.

In this study physical concepts and equations were used to model the combustion phenomenon in an RCCI heavy-duty engine. One of the main goals in this research is to predict CA50 as a property of in-cylinder combustion. The majority of the models that used Arrhenius method were done for the engines with one fuel. However, COM was used for modeling of the RCCI engine combustion which works with two fuels such as gasoline as LRF and diesel as HRF which are also considered in MKIM equations. In fact, this type of combustion is related to fuel mixture reactivity and the oxygen concentration [17, 21]. Calibration and validation of modeling is performed using five experimental data type those are various in variation of input parameters, about 5000 cycles data points. Calibration was applied on three data sets and in validation section two data sets plus these three data sets were used. In fact, constants of calibration were applied on all data sets. In each section there are some constant values which are obtained from calibration data sets. Intake pressure (Pint), gasoline fraction(GF) and exhaust gas recirculation (EGR) have been changed in experimental data series. Start of combustion (SOC) was modeled with MKIM method using a time function which contains the effects of the engine operating conditions such as fuels mixture, EGR, and fuel mixture reactivity (Cetane number of the fuels). Modeling of burn duration (BD) is performed using the effect of spontaneous front speed considering all effective parameters. A relation between burn duration and spontaneous front speed was then obtained using material derivation on time equation. Wiebe function is used for the CA50 modeling. The main contribution in this research is providing a control oriented method based on a new delay time function (time between SOI and start of combustion) of engine operational conditions such as fuels equivalence ratios, oxygen concentration (which provides different delay time function) to have a prediction on combustion characteristics such as SOC, burn duration and CA50 in an RCCI engine, the method of expanding COM was also improved and updated. Start of combustion estimation that can be used as a factor of analysis engine behavior such as engine efficiency, fuel consumption, emissions and etc. CA50 also have same condition as SOC and is predicted in this research similar to burn duration. Figure 1 shows the block diagram of model estimation.

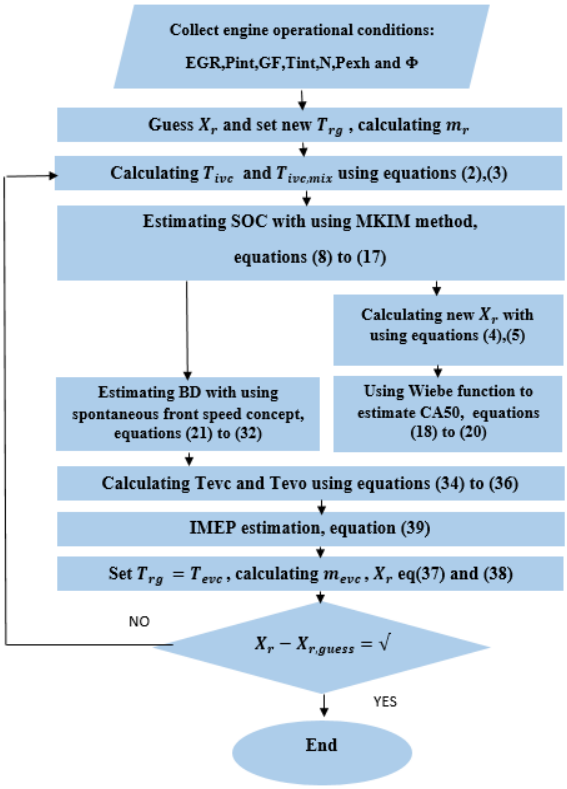

Figure 1: Block diagram of the estimation method

2. Experimental setup

Experimental data has been used to develop MKIM. These data obtained from a heavy-duty engine that is modified to run at RCCI mode operation. Each cylinder equipped with a direct injection injector which injects diesel into the cylinder and a port fuel injector that injects low reactivity fuel into the intake manifold. To expand the engine operational domain and to increase efficiency, compression ratio of each cylinder is reduced to a lower amount by doing some changes in the engine piston. Table 1 shows this engine specification.

Table 1 : Engine specifications

Engine specification	
Number of cylinder	**6**
Bore x stroke	**110mm x 135mm**
crank Length	**67.5 mm**
Total displacement	**7700 cm2**
Compression Ratio (Nominal)	**17.5:1**
Compression ratio (RCCI configuration)	**12.2:1**

Moreover, some ordinary sensors are used to obtain necessary data such as temperature, pressure and air intake flow rate from the engine. A Kistler 6125C pressure transducer is used to determine in-cylinder pressure. For measuring engines emissions, a Horiba Mexa-One was used. Also, another sensor determines

concentration of CO_2 in intake air mixture ($[CO_2]_{int}$). EGR has been calculated with Eq.1 that is used in [5]:

$$EGR = \frac{[CO_2]_{int} - [CO_2]_{atm}}{[CO_2]_{exh} - [CO_2]_{atm}} \quad (1)$$

$[CO_2]_{atm}$is concentration of CO_2 in atmosphere and equals to 0.04%. In this experimental setup commercial gasoline was used as low reactivity fuel that is injected from air intake manifold and entered the cylinder; diesel used as high reactivity fuel that is injected directly to each cylinder [5].

Injection control is performed using a real-time National Instruments controller (PXIe-8135) and an embedded Field Programmable Gate Array (FPGA) chassis with dedicated modules (NI-9155). The acquisitions of signals were carried out by a 16-analog-channel acquisition card (PXIe-6358). Figure 2 shows experimental setup of this research.

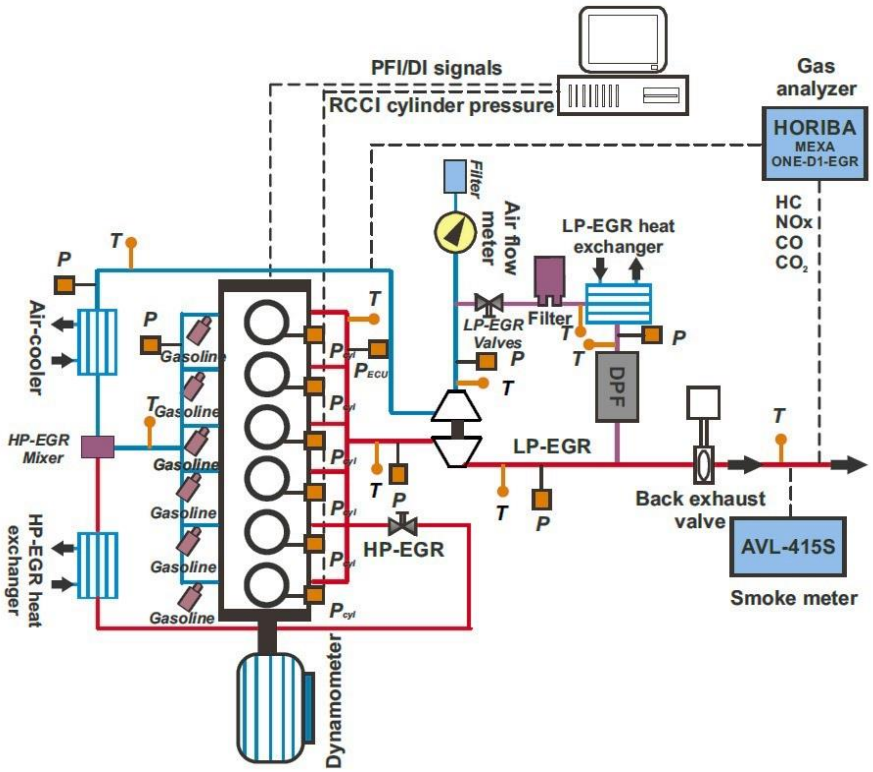

Figure 2: Experimental setup

In the experimental data recorded the injection was controlled cylinder-to-cylinder in order to ensure a similar combustion trend. The distribution of the fresh air was considered to be uniform within the intake manifold while the EGR was performed using only low-pressure EGR to ensure a proper mixing of the recirculated gases and thus limit an eventual cylinder-to-cylinder dispersion. For each operational condition there are about 4981 data points in 18 data sets, those collected from a six-cylinder Volvo engine and a mean value of each cycle obtained from six cylinders and used as an input for the calibration of the model.

For each data point there are about 230 cycles, calculating standard deviation, Figure 3 shows cycle to cycle variation of data for IMEP and CA50, according to this figure maximum deviation for IMEP is about 0.0982 bar and this parameter is about 0.638 CAD for CA50 experimental data. Selecting data is based on previous

research works and are in direction of the effective parameters on engine operation. Because of the number of iteration in each data sets there is enough accuracy for each combustion characteristics.

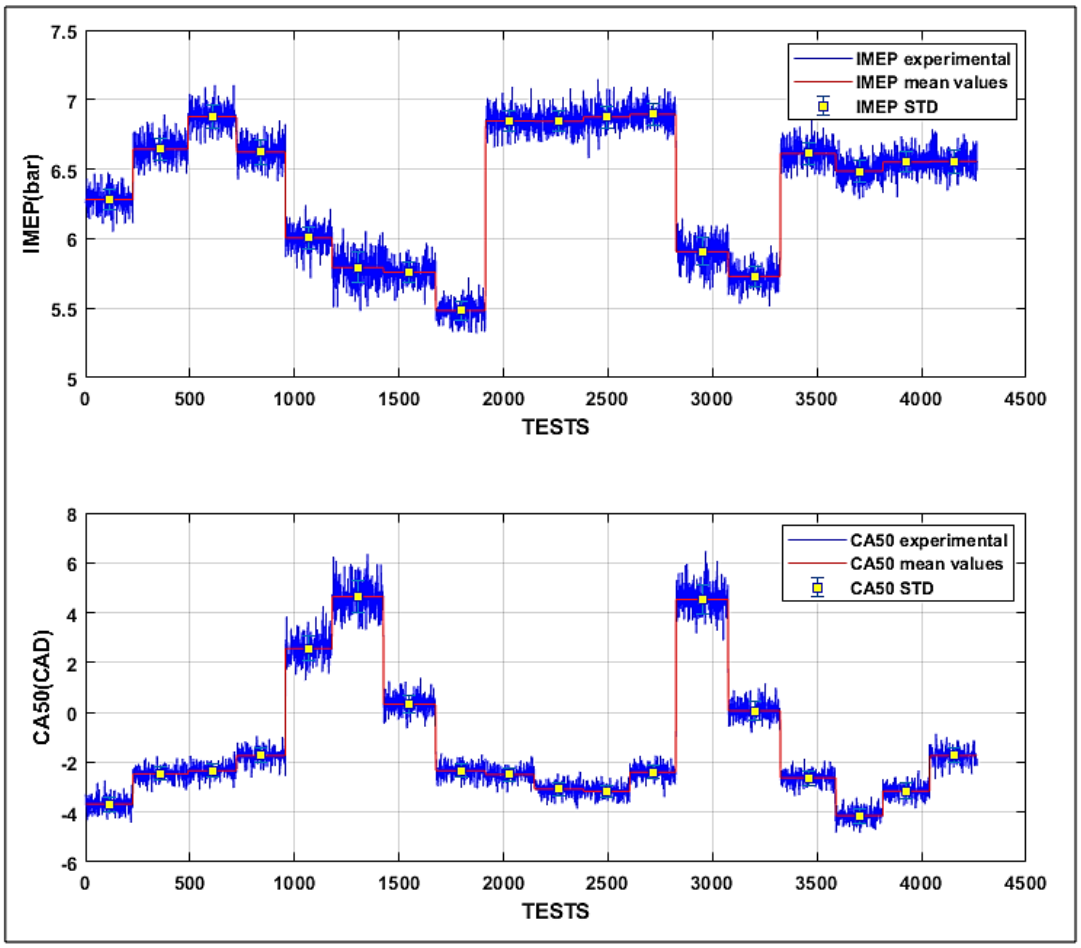

Figure 3: cycle to cycle variation of experimental data

3. Combustion modeling

Control oriented method (COM) was used to develop modeling of combustion in a reactivity control compression ignition engine. The main purpose was modeling SOC, BD, CA50 and IMEP which are properties of the combustion in IC engines. In this research COM is divided into different parts, from inlet valve close (IVC) to start of combustion (IVC to SOC), BD which is from SOC to the end of combustion(EOC). For obtaining conditions at exhaust valve closure (EVC) it was needed to model in-cylinder process from EOC to exhaust valve opening (EVO) and from EVO to EVC, with these estimations of in-cylinder process indicated mean effective pressure(IMEP) which is a property to have control on engine power and efficiency, has been also modeled. CA50 as it was said before is an angle which 50% of fuel burns was also modeled in this research.

3.1. IVC conditions

As explained before, IVC conditions in combustion modeling are very important because of their usage in MKIM [26]. The residual in-cylinder gasses with a specific temperature have impact on IVC conditions. Temperature of IVC can be written as below [5,17]

$$\mathrm{T_{ivc_1}} = \frac{\mathrm{P_{ivc}}.\mathrm{V_{ivc}}}{\mathrm{m_{cyl}}.\mathrm{R}} \tag{2}$$

$$\mathrm{T_{ivc,mix_i}} = \mathrm{T_{ivc_i}}\left(1 - X_{rg_{i-1}}\right) + T_{rg_{i-1}} X_{rg_{i-1}} \tag{3}$$

X_r is residual gas mass fraction, T_{rg} is temperature of residual gasses.

$$X_r = \overbrace{\sqrt{\frac{1}{C}\frac{\pi\sqrt{2}}{360}\frac{r_c-1}{r_c}\frac{OF}{N}\sqrt{\frac{RT_{int}|P_{exh}-P_{int}|}{P_{exh}}}\left(\frac{P_{exh}}{P_{int}}\right)^{\frac{k+1}{2k}}}}^{\alpha} + \overbrace{\frac{1}{C}\frac{r_c-1}{r_c}\emptyset_{tot}\frac{V_{ivo}}{V_{dis}}\left(\frac{P_{exh}}{P_{int}}\right)^{\frac{1}{k}}}^{\beta} \tag{4}$$

OF is the valve overlap factor that is calculated using geometry and the timing of both intake and exhaust valves. The parameter C is calculated as below [17,29]:

$$C = \left[1 + \frac{LHV}{c_v T_{int}\left(\frac{m_t}{m_f}\right) r_c^{k-1}}\right]^{\frac{1}{k}} \tag{5}$$

$$m_t = m_a + m_f + m_{rg} + m_{egr} \tag{6}$$

LHV represents the lower heating value of the fuel. The valve overlap in this type of engine is about zero, so the first section of equation 4 (α) is negligible and was assumed to be zero. In the first stage of calculation, X_r , T_{rg} have been guessed; after that m_{rg} was calculated from equation 7 [16] and new X_r , T_{rg} were obtained at the end of each stage of calculation.

$$X_r = \frac{m_{rg}}{m_t} \tag{7}$$

3.2. IVC to SOC

It was assumed that compression process in this modeling follows polytropic relationship and therefore in-cylinder pressure and temperature were calculated from equations (8) and (9) [5].

$$\mathrm{P}(\theta) = \mathrm{P_{ivc}}\left(\frac{\mathrm{V_{ivc}}}{\mathrm{V}(\theta)}\right)^{\mathrm{k}} \tag{8}$$

$$\mathrm{T}(\theta) = \mathrm{T_{ivc}}\left(\frac{\mathrm{V_{ivc}}}{\mathrm{V}(\theta)}\right)^{\mathrm{k-1}} \tag{9}$$

It has been assumed that k is a constant.

MKIM was used to estimate SOC, this integral starts from IVC to the point that SOC will happen. if it was is assumed that amount of this equation equals to one with enter constant A to left hand side of equation (10) [16]:

$$\int_{\theta_{ivc}}^{\theta_{soc}} \frac{1}{A*N*\exp\left(\frac{b}{T(\theta)}P(\theta)^n\right)} = 1 \quad (10)$$

In equation (10) b, A and n should be calibrated and N is engine speed in rpm. T and P are the temperature and pressure respectively in each crank angle degree (CAD).

b is related to fuel energy of activation (Ea) which is calculated by Ea/R [14]. Because of using two fuels in RCCI engines Ea depends on energy activation of two fuels and is calculated as follow [16]:

$$Ea = c_1/(CN_{mix} + c_2) \quad (11)$$

Equation (12) shows the formula for CN_{mix}, which is Cetane number of fuel mixture,

$$CN_{mix} = GF.\,CN_{pfi} + (1 - GF).\,CN_{di} \quad (12)$$

Gasoline fraction (GF) is the fraction of fuel that is injected to inlet port which is calculated as $GF = m_{pfi}/m_{fuel}$. CN_{pfi} and $CN_{di}$are Cetane numbers of port fuel injection (PFI) and diesel which is direct injected fuel.

As mentioned in previous sections, combustion is related to the fuel mixture and inlet oxygen. φ_{DI} and φ_{PFI} are concentration of Diesel and gasoline, respectively.$[O_2]_{int}$is calculated from equation (13).

$$[O_2]_{int} = [O_2]_{atm}\,.\,(1 - EGR) - [O_2]_{exh}\,.\,EGR \quad (13)$$

$[O_2]_{atm}$is the oxygen of atmosphere which is assumed at 21%. with equation (13) it can be concluded that A also depends on global equivalence ratio of diesel (φ_{DI}) , global equivalence ratio of port fuel injection (φ_{PFI}) and exhaust gas recirculation(EGR) [16]. In equation 10, A is a constant that can represent the role of input variables on combustion characteristic, so A was written as equation 14, in this equation $[O_2]_{int}$, intake oxygen, that was obtained from equation 13 contains other operational conditions variables effects; such as EGR , exhaust oxygen ($[O_2]_{exh}$) and $[O_2]_{atm}$ .Although global equivalence ratios contain intake oxygen effects, intake oxygen was used in equation 14 to investigate direct effect of intake oxygen on delay time function. In fact, using intake oxygen is a way to have EGR effect on ignition delay time.

$$A = a_1\left(\varphi_{DI}^{a_2} + \varphi_{PFI}^{a_3} + {[O_2]_{int}}^{a_4}\right) \quad (14)$$

Therefore, MKIM is calculated with equation 15:

$$\int_{\theta_{ivc}}^{\theta_{soc}} \frac{d\theta}{\underbrace{Na_1\left(\varphi_{DI}^{a_2}+\varphi_{PFI}^{a_3}+{[O_2]_{int}}^{a_4}\right)\left(\frac{c_1/(CN_{mix}+c_2)}{RT(\theta)}P(\theta)^n\right)}_{\tau}} = 1 \quad (15)$$

$a_1, a_2, a_3, a_4, c_1, c_2$, n are constants which are calibrated from experimental data. In equation (15) τ is a function of delay between IVC and SOC [15] which is calculated as.

$$\tau = Na_1\left(\varphi_{DI}^{a_2} + \varphi_{PFI}^{a_3} + {[O_2]_{int}}^{a_4}\right)\left(\frac{c_1/(CN_{mix}+c_2)}{RT(\theta)}P(\theta)^n\right) \quad (16)$$

It was assumed that direct injected fuel is mixed well with the mixture of LRF and air. Therefore, the time of this mixing process is negligible and as a result fuels in combustion of RCCI engines are premixed and lean. Whit this assumption, combustion depends on the chemical condition rather than physicals. Time equation can be written as (17)

$$t = \tau\left(\varphi_{DI}, \varphi_{PFI}, [O_2]_{int}, CN_{mix}, T(\theta), P(\theta)\right) \quad (17)$$

Generally, delay time for each spontaneous or non-spontaneous phenomenon from condition 1 to condition 2 can be written as:

$$t = \tau(x_1, x_2, x_3 x_4, x_5, x_6, \dots\dots, x_n) \quad (18)$$

3.3. CA50 modeling

CA50 is the angle where 50 percent of the fuel burns. Wiebe function is used to model CA50. [20]

$$x_b = 1 - exp\left(-a\left[\frac{\theta-\theta_{soc}}{\theta_d}\right]^{m+1}\right) \quad (19)$$

In Wiebe function, equation (19),x_b is fraction of fuel burnt in each CAD and θ_d is burning duration in CAD, equation 20 [21].This relation of burn duration shows dependency of combustion duration to different input variables such as global equivalence ratio of each fuels and dilution factor, dilution factor represents both EGR and residual gasses and depends on valve timing, engine speed, fuel amount, intake manifold pressure and exhaust manifold pressure was calculated from equation 21[20]. Using equation 20 to model CA50 provides more mathematically control on direct calibration of CA50 which was used also by A. Raut, et al, in 2018 [38]

$$\theta_d = C(1 + x_d)^D(\varphi_{DI}^{b_1} + \varphi_{PFI}^{b_2}) \quad (20)$$

In equation 21 ,x_d is the dilution factor, [29]. C, d, m, a, b_1 and b_2 should be calibrated from experimental data [20].

$$x_d = EGR + \frac{X_r}{1-X_r} \quad (21)$$

3.4. Burn Duration modeling

The start of combustion in RCCI engines can be varied due to input engine conditions and also start of ignition (SOI), in previous section effects of input condition were discussed and used in modeling of SOC. start of injection also influence on start of combustion, in all SOI conditions the process almost is same, in early SOI combustion will occur because of compression and in the way of auto-ignition. In late SOI there is also a delay from SOI to SOC due to auto-ignition process. As mentioned before, in RCCI engines, combustion is a lean type and therefore flame propagation is not effective on BD [16]. the main reason of this phenomenon is combustion conditions which are below flame occurrence standards there is an exception in high load of engine operation [16]. In this research because of low load engine in experiments, it was assumed that flame propagation does not impact on combustion process.

As high reactivity fuel is injected to the cylinder some reactions are produced in different layer of fuel mixture (in all volume of it). This causes starting an ignition with spontaneous front speed which is a N-

variable function that is effective on combustion duration in all over the fuel mixture, according to combustion occurrences in random points so locations of these reactions are not clear which makes their prediction a very difficult task [16].

According to τ equation (17,18), delay time depends on different variables; if it is assumed $\vec{V}$ is spontaneous front speed of ignition that is effective on start of combustion delay. Using material derivation on equation (17,18), it can be obtained mathematically:

$$\frac{Dt}{Dt} = \overset{t=\tau}{\Longrightarrow} = \frac{\partial \tau}{\partial t} + \vec{V}.(\nabla \tau) \tag{22}$$

According to equation (17,18), τ does not depend on time and therefore $\frac{\partial \tau}{\partial t} = 0$ and $\frac{Dt}{Dt} = 1$

$$1 = \vec{V}.(\nabla \tau) \tag{23}$$

$$\vec{V} = \frac{1}{\nabla \tau} \rightarrow \left|\vec{V}\right| = S_{ig} = \frac{1}{|\nabla \tau|} \tag{24}$$

$S_{ig}$is spontaneous front speed that was used also in previous researches [16, 28,35] for BD modeling.

$$\tau = ANexp\left(\frac{b}{T(\theta)}P(\theta)^n\right) = Na_1\left(\varphi_{di}^{a_2} + \varphi_{pfi}^{a_3} + [O_2]_{int}{}^{a_4}\right)\exp\left(\frac{C_1}{R(CN_{mix}+C_2)}\frac{1}{T(\theta)}P(\theta)^n\right) \tag{25}$$

$$\tau = f\left(\varphi_{di}, \varphi_{pfi}, CN_{mix}, T, P, [O_2]_{int}\right) \tag{26}$$

Therefore

$$|\nabla \tau| = \sqrt{\left(\frac{\partial \tau}{\partial \varphi_{di}}\right)^2 + \left(\frac{\partial \tau}{\partial \varphi_{pfi}}\right)^2 + \left(\frac{\partial \tau}{\partial CN_{mix}}\right)^2 + \left(\frac{\partial \tau}{\partial T}\right)^2 + \left(\frac{\partial \tau}{\partial P}\right)^2 + \left(\frac{\partial \tau}{\partial [O_2]_{int}}\right)^2} \tag{27}$$

According to equation (25) $T(\theta)$ and $P(\theta)$ should be estimated for calculating each partial derivative part in equation (27). As S_{ig} becomes conceptualized from SOC, temperature and pressure were used for modeling of burn duration, T_{SOC} and P_{SOC}. The formulas for estimating corrected temperature and pressure (T_C and P_C) are as follow: [16,19]

$$T_c = T_{soc} + e_1 \Delta T \tag{28}$$

$$P_c = P_{soc} + e_2 \Delta T \tag{29}$$

$$\Delta T = \frac{Q_{LHV,di}FAR_{st,di}\varphi_{di} + Q_{LHV,pfi}FAR_{st,pfi}\varphi_{pfi}}{c_v\left(FAR_{st,di}\varphi_{di} + FAR_{st,pfi}\varphi_{di} + 1\right)} \tag{30}$$

$$e_1 = d_0 + d_1 SOC + d_2 SOC^2 \tag{31}$$

$$e_2 = f_0 + f_1 SOC + f_2 SOC^2 \tag{32}$$

As it was said before, combustion in RCCI engines comes from spontaneous ignition in all the volume of fuel mixture, BD is a function of spontaneous front speed [16,19].

$$BD = K_1(S_{ig})^{\zeta} \quad (33)$$

$d_0, d_1, d_2, f_0, f_1, f_2, K_1, \zeta$ are constant which are used in equations (28) to (33) and should be calibrated from experimental data sets.

3.5. EOC estimation

As SOC and BD was modeled in previous sections, end of combustion will be estimated as follow:

$$EOC = BD + SOC \quad (34)$$

3.6. Polytropic expansion ($EOC \rightarrow EVO$)

Using polytropic formulas, temperature and pressure at EVO will be modeled as follow: [38].

$$T_{evo} = T_{eoc}\left(\frac{V_{eoc}}{V_{evo}}\right)^{n_e-1} \quad (35)$$

$$P_{evo} = P_{eoc}\left(\frac{V_{eoc}}{V_{evo}}\right)^{n_e} \quad (36)$$

Where n_e is the polytropic expansion coefficient and is calculated from the experimental data.

3.7. Exhaust stroke ($EVO \rightarrow EVC$)

The process from opening exhaust valve to the time of closing was modeled using polytropic process [14]. As the result of this assumption, temperature at EVC is calculated from Equation 37. It was assumed that this temperature is the same as residual gas temperature [38]:

$$T_{evc} = T_{evo}\left(\frac{P_{exh}}{P_{evo}}\right)^{\frac{n_e-1}{n_e}} \quad (37)$$

It is assumed that the mixture of exhaust gas at EVC obeys the ideal gas law, so the mass of residual gasses will be as follow [38]:

$$m_{evc} = \frac{P_{exh}.V_{evc}}{R_{evc}.T_{rg}} \quad (38)$$

Where R_{evc} is gas constant for EVC condition and $T_{rg} = T_{evc}$. The residual mass fraction is calculated from Equation 39:

$$X_r = \frac{m_{evc}}{m_{tot}} \quad (39)$$

calculations were continued until X_r converge.

3.8. IMEP modeling

The integral of pressure times volume on entire engine cycle was used to calculate IMEP. A temperature variation was used to calculate IMEP considering some assumptions [38]. Equation 40 is used to calculate IMEP as follow:

$$IMEP = Bm_t \frac{c_v}{V_{dis}} \left(T_{ivc,mix} - T_{soc} + T_{eoc} - T_{evc}\right) \quad (40)$$

B is the correction factor which is used to adjust the delta between modeling assumptions and the actual conditions. Its final value is calibrated from the experimental data.

4. Experimental data

Five series of distinct data set those are generated by changing input condition parameters such as P_{int}, GF and EGR were used . Note that the engine speed is constant in all data type set and is set at 1200 rpm. For each data type set the apparent heat release rate,$AHRR$, can be calculated from equation (41) as follow :

$$AHRR(\theta) = \frac{k}{k-1}.P(\theta)dV(\theta) + \frac{1}{k-1}V(\theta)dP(\theta) \quad (41)$$

It was assumed that k is 1.35. The use of such model with a constant k is fast for real-time application and precision was found to be sufficient for this application. Such statement was also studied in J. Bengtsson et al. [39] where the AHRR was named net heat release showing that a simple model as the one used in this work with a constant polytropic index gave similar accuracy to more complex models regarding CA50 calculation.

As mentioned before, there are five different experimental data sets, three of them were used for calibrating and the results were applied to all five data-set for validation. Operational conditions for first three data sets are shown in table 2.

Table 2: first three data set using in calibration section

Test cases operational conditions												
specification	**Case1**				**Case2**				**Case3**			
Pint(bar)	1.65	1.42	1.37	1.28	1.18	1.18	1.18	1.18	1.38	1.38	1.38	1.38
GF	0.456	0.456	0.454	0.455	0.509	0.581	0.394	0.278	0.450	0.450	0.450	0.450
EGR	0	0	0	0	0	0	0	0	0.5	4.5	11.5	21
SOI main (CAD bTDC)	50	50	50	50	50	50	50	50	50	50	50	50
SOI pilot (CAD bTDC)	60	60	60	60	60	60	60	60	60	60	60	60
Tint (k)	315.4	314.1	313	313.2	315	314.1	314.8	314.5	314.5	314.5	314.5	314.5
Ambient Pressure (bar)	1	1	1	1	1	1	1	1	1	1	1	1
Ambient Temp(k)	300	300	300	300	300	300	300	300	300	300	300	300
number of iteration	227	262	231	233	223	271	249	237	233	233	221	220
engine speed(rpm)	1200	1200	1200	1200	1200	1200	1200	1200	1200	1200	1200	1200

Figure 4 also shows the variation of these data in each test case point. Number of iteration is number of measuring each operational condition, for example Pint=1.65 in case1 measured 227 times.

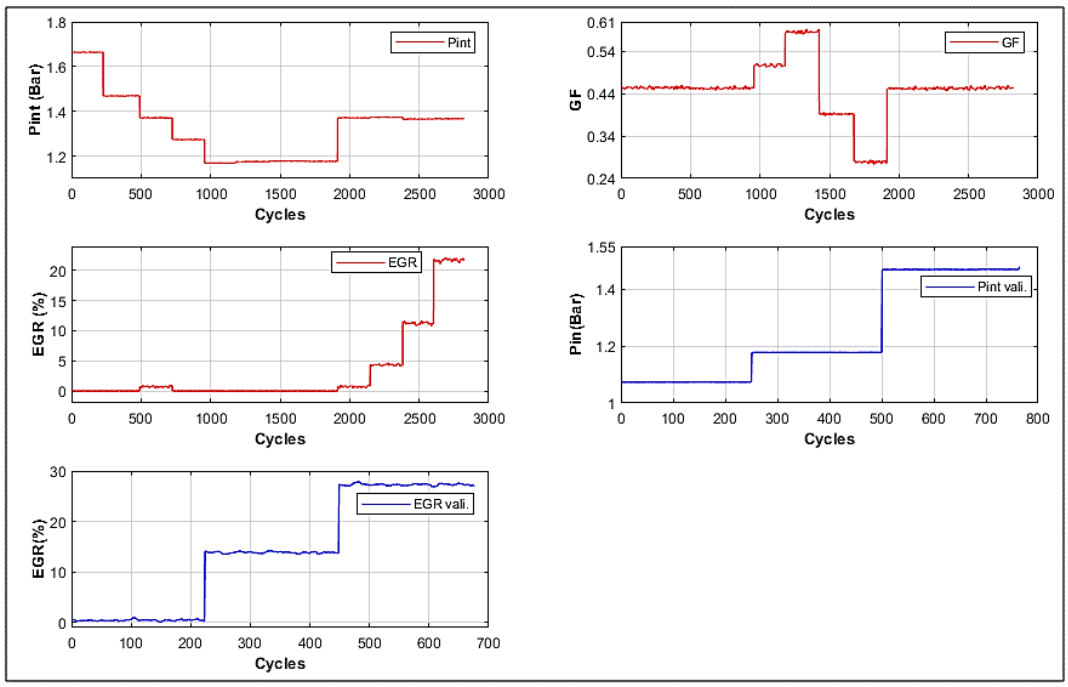

Figure 4: Five different data types used for calibration and validation process

Table 3 shows two other data-set types used for validation beside previous data sets.

Table 3 : operational condition for validation data

Test cases operational conditions						
specification	**Case4**			**Case5**		
Pint(bar)	1	1.18	1.45	1.47	1.47	1.47
GF	0.5	0.4	0.45	0.4	0.4	0.4
EGR	0	0	0	0	14	28
SOI main (CAD bTDC)	50	50	50	50	50	50
SOI pilot (CAD bTDC)	60	60	60	60	60	60
Tint (k)	314.2	315.3	314.1	314.1	314.3	314.3
Ambient Temp(k)	306	306	306	306	306	306
Number of iteration	250	246	264	224	224	225
Engine speed(rpm)	1200	1200	1200	1200	1200	1200

5. Transient data set

In addition to five data type series used for calibration and validation (Figure 4) in steady state condition, the constants were also applied to a transient condition data series, Figure 5. As it is shown in Figure 5 there is a suddenly change into GF, P_{int} and EGR which because of applying changes in the input engine variables. GF was changed from 0.45 to 0.63, where these changes are 1.27 bar to 1.37 bar for P_{int} and 20% to 33%

of EGR. Also there is a small change in engine speed at start and end of applying changes, it was assumed that engine speed is constant and is 1200rpm.

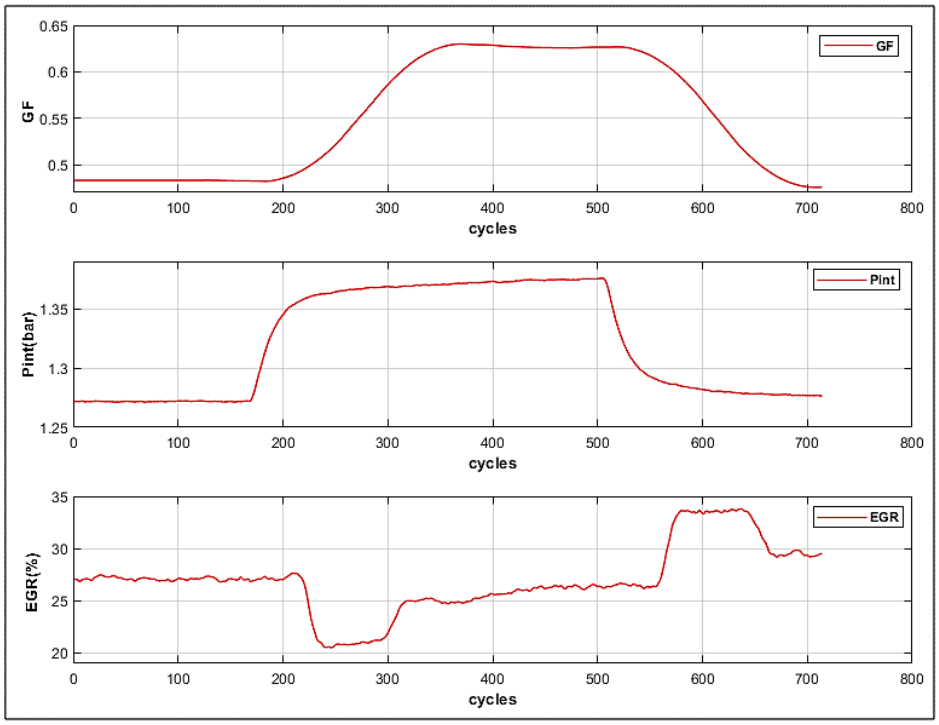

Figure 5: Transient experimental data set.

6. Calibration and validation

6.1. SOC calibration and validation

In low temperature engines specially in RCCI engines, heat release takes place in two steps which are (i) low temperature heat release (LTHR) and (ii) high temperature heat release (HTHR). In this study, SOC is a point on AHRR where second stage of the heat release begins. First three data sets were applied on equation (16) which is a type of MKIM. Constants in this equation are calibrated using a MATLAB program. Matlab code algorithm is based on finding the minimum of difference between experimental data and mathematical model. P_{int}, EGR and GF data series were used to calibrate n , C_1,C_2 ,a_1 *to* a_4 . Constants after calibration are shown in Table 4.

Table 4 : Constants calibrated for SOC from MKIM

n	C_1	C_2	a_1	a_2	a_3	a_4
1.7e-06	-7.8e-08	-0.1031	1. e-05	1.4343e+10	644.5756	-0.1553

The result of applying constant on all data series for estimation of SOC was illustrated in Figure 6. This SOC estimation is compared against the experimental data in this figure. Occurrence distribution of

estimated value was also showed in Figure 6. As shown in this figure, most of data estimation have error less than 1.5 CAD.

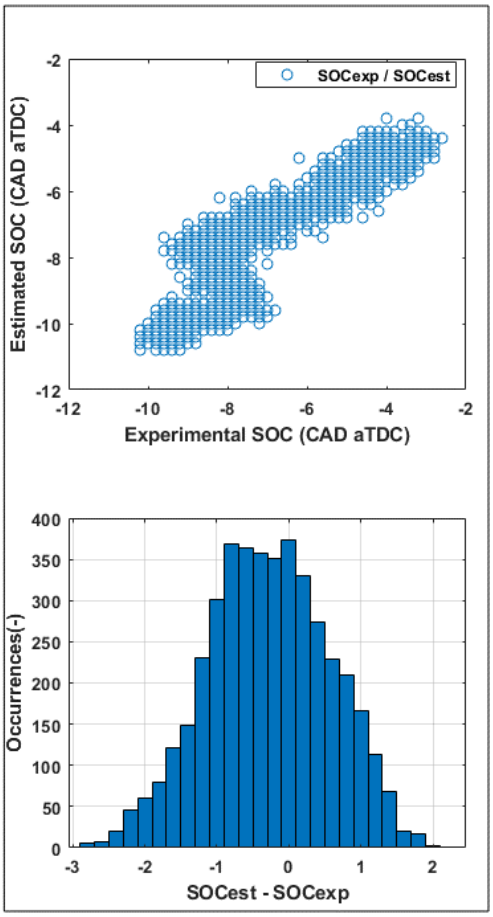

Figure 6: SOC estimation compared to experimental data, data occurrences distribution

Mean error of estimated SOC is shown in Figure 7; maximum mean error is in EGR data set and is about 1.7 CAD. In addition to the low mean error there is a good trend in the validation and estimation. This figure also shows cycle to cycle change of experimental and estimated SOC beside error bars for each mean values.

Among 18 data point sets there is only one data point set which has mean error more than 1.1 CAD, all other errors are below and around 1 CAD. Figure 7, although 1.7 CAD is an acceptable error with considering this fact that estimated and experimental diagrams are in same directions.

This error also shows that difficulty of EGR calibration in this type of time equation is higher than other operational conditions for combustion start estimation.

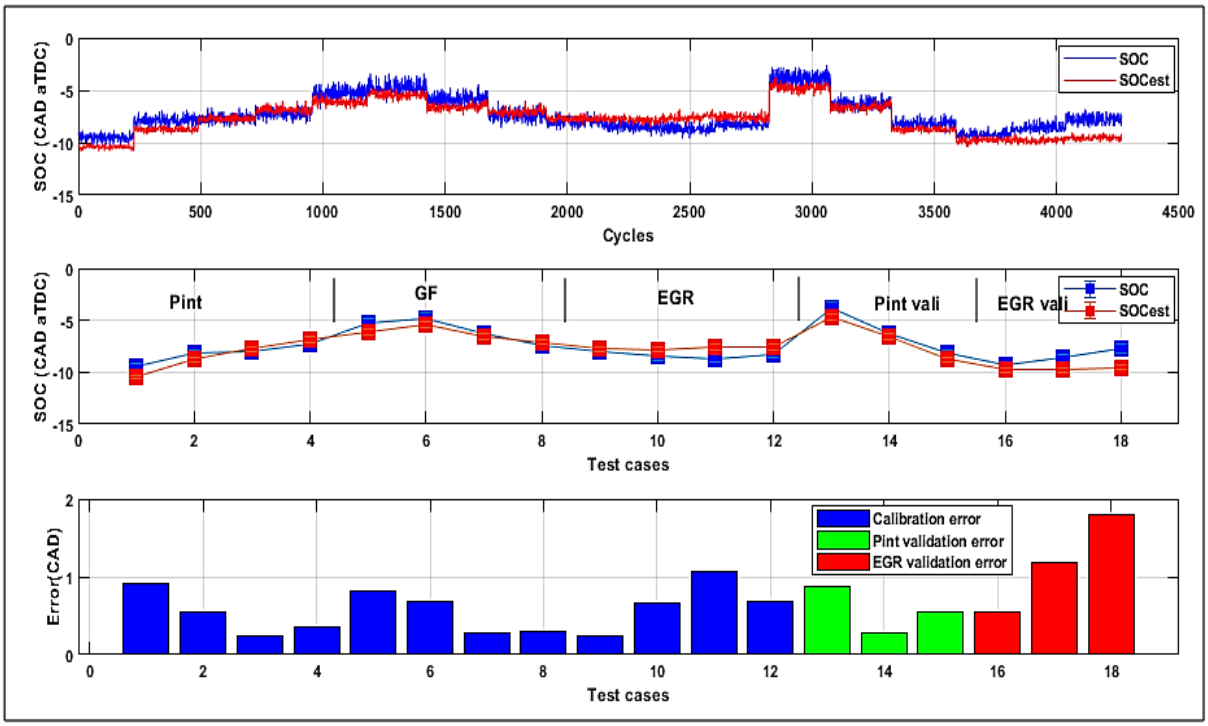

Figure 7 : SOC estimation and validation, cycle to cycle SOC, mean values and error bars

In equation (17) which is the time between IVC to SOC, EGR was applied using O_{2int} in a polynomial equation. Nevertheless, it seems that combustion process was influenced by heating values of the full fuel mixture. Since the EGR has non effective heating value so it has less effect on total heating values, as a result estimation of SOC in EGR sections (points from 9-12 and 16-18) could not capture the trend perfectly but there are low mean errors in these sections.

6.2. CA50 calibration and validation:

As discussed, Wiebe function is used to model CA50 using equations (19-21). According to these equations C, d, m, a, a_1 and a_2 should be calibrated. Using three data type set to calibrate CA50, the coefficients have been obtained as Table 5.

Table 5 : Calibration CA50 constants

C	D	b_1	b_2	a	m
5.4938	-0.0067	0.0273	-43.8397	135.759	-158.3813

By applying the coefficients to equations (19-21) CA50 will be estimated. Figure 8 shows difference between CA50 estimation and CA50 experimental. As shown in this figure occurrences of this method in most of data point have an error less than 1.5 CAD.

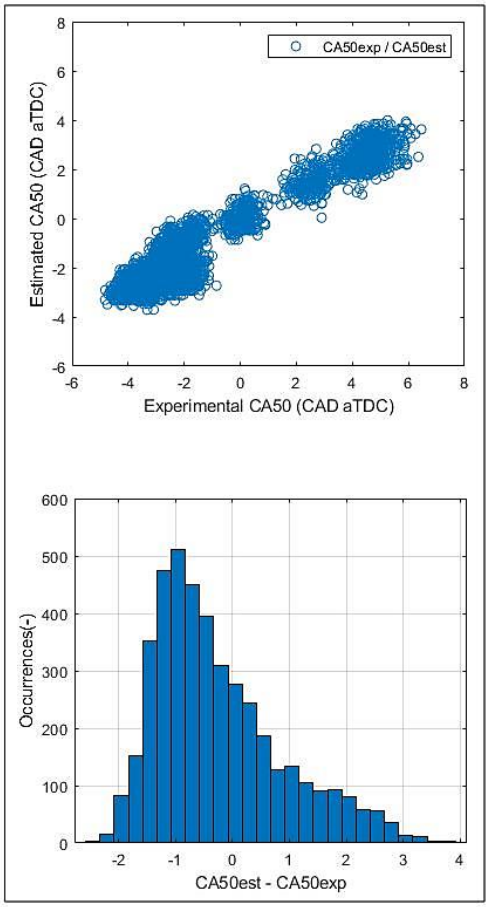

Figure 8 : CA50 estimation compared to CA50 estimation. data occurrences distribution

According to Figure 8 there are acceptable accuracy in data estimation. Beside this, Figure 9 shows cycle to cycle estimated CA50 and experimental data, difference between mean values of estimated and experimental CA50 beside error bars for each data point. The maximum error is about 2.3 CAD. this diagram also shows a good correlation between estimated CA50 and the experimental one. All mean errors are less than 1 CAD except one point that is related to gasoline fraction estimation, although this error is higher than other point error but direction of estimated diagram is in experimental data direction.

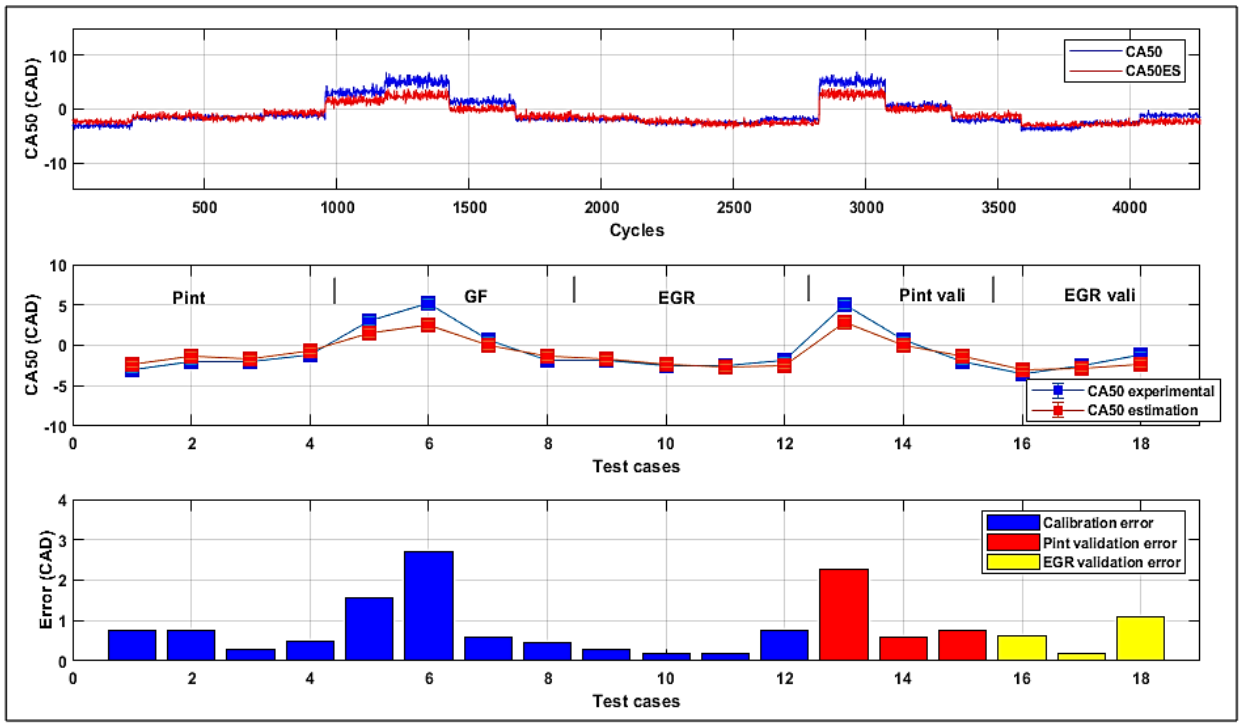

Figure 9: CA50 estimation and validation, cycle to cycle CA50, mean values and error bars

6.3. BD calibration and validation

Burn duration was considered from start of combustion to CA90, in fact, CA90 was calculated from cumulative heat release (CHR) which is 90 percent of maximum CHR. With this assumption, experimental BD was obtained. By applying calibration data on BD equations in the model the coefficients on BD estimation are obtained which are shown in Table 6.

Table 6 : BD estimation constants obtained from MATLAB coding

K_1	ζ	d_0	d_1	d_2	f_0	f_1	f_2
1860.34	0.1962	-12.603	0.03749	0.0027	-1.363	28.570	21.13

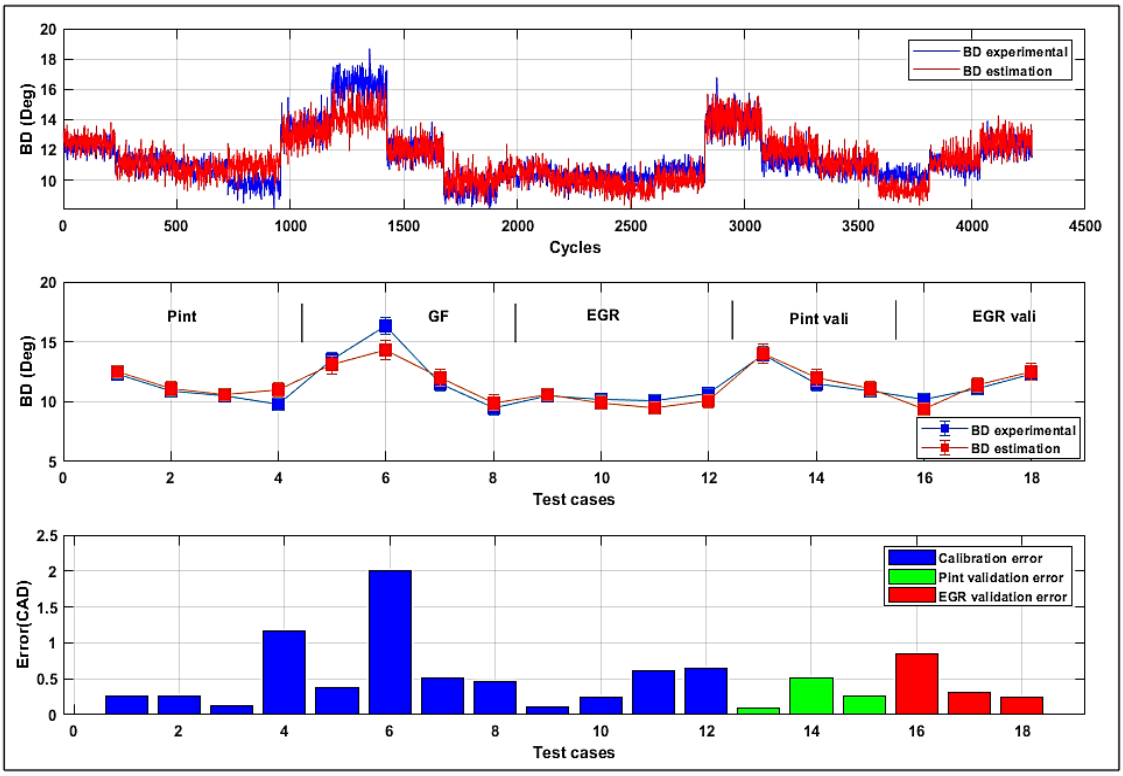

Figure 10: BD estimation and validation, cycle to cycle BD, mean values and error bars

Applying constants on all data series shows acceptable trend in BD estimation where maximum mean error is about 1.9 CAD that is related to data case number six from GF calibration data. According to experimental data of GF all datasets have GF below or equal to half except one data set which is about 0.6. Calibration model has better result for $GF \leq 0.5$ and for above this fractions mean error becomes higher. This can be a result of too much non-linearity of reaction related to GF in real cylinder while in this COM solution GF was applied to the estimation in equation (17) in a polynomial linear equation form. This is also true for CA50 modeling in the dataset 6. Despite of this, there is a good trend in this point of calibration. All other mean errors are less than 2 CAD. Figure 10 shows comparison between the experimental BD and estimated BD in mean values this figure also compares cycle to cycle estimation and validation data, error bars for each mean values also was illustrated in this figure. Data distribution accuracy for BD is shown in Figure 11. Most of the estimated data error are less than 2 CAD.

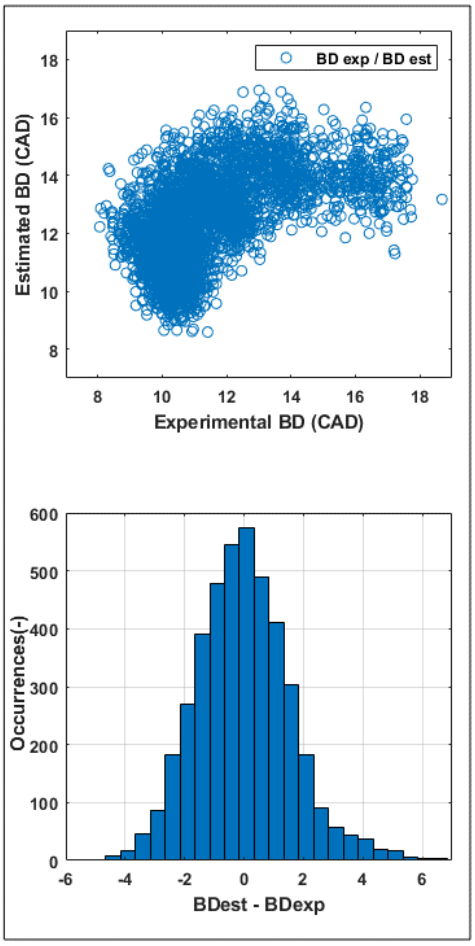

Figure 11: Experimental and estimation BD comparison, data occurrences distribution

6.4. IMEP estimation

IMEP was estimated with equation 40, in this way EOC was obtained from equation (34). $\boldsymbol{n_e}$ that is used in equations 35 to 37 has been calculated from experimental data and is 1.28, $\boldsymbol{B}$ was obtained 1.49 and was used in equation 39 to calculate IMEP. Figure 12 shows contribution of estimated IMEP comparting with experimental IMEP, as it is clear in this Figure error of IMEP estimation are below 0.5 bar.

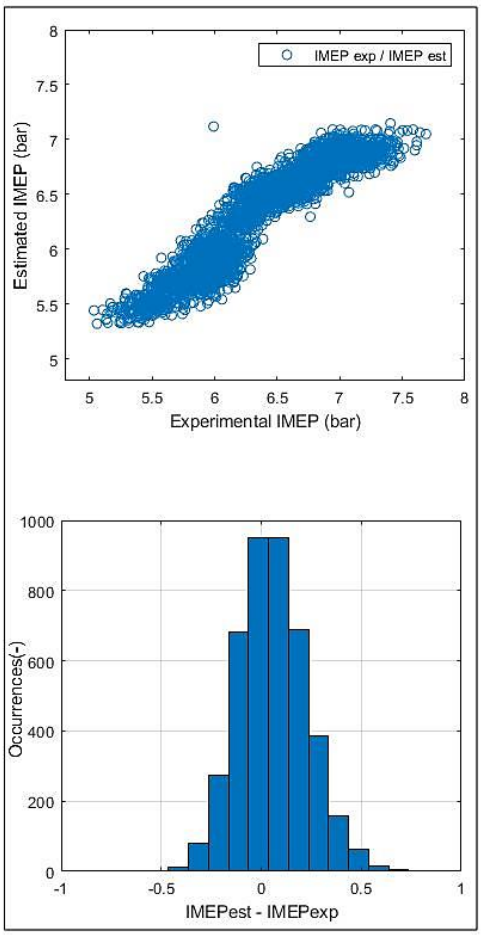

Figure 12: Experimental and estimation IMEP comparison, data occurrences distribution

Comparing IMEP estimation in mean error with experimental IMEP shows mean error below 0.45 bar, beside this as it was shown in Figure 13 there is also an acceptable trend in estimation of IMEP. Maximum mean errors related to IMEP estimation in EGR section which due to SOC estimation, SOC temperature was used in estimation of IMEP, equation (40), this figure also shows changing in EGR has no effects on IMEP of the engine and as a results it has no effective role on engine output power. Cycle to cycle calibration and validation data beside error bars also were showed in this figure.

As it was discussed above maximum mean error in IMEP validation is below 0.45 bar, also there is a point with about 1.3 bar error but in this research because of high number of iterations mean values considered as comparable factors.

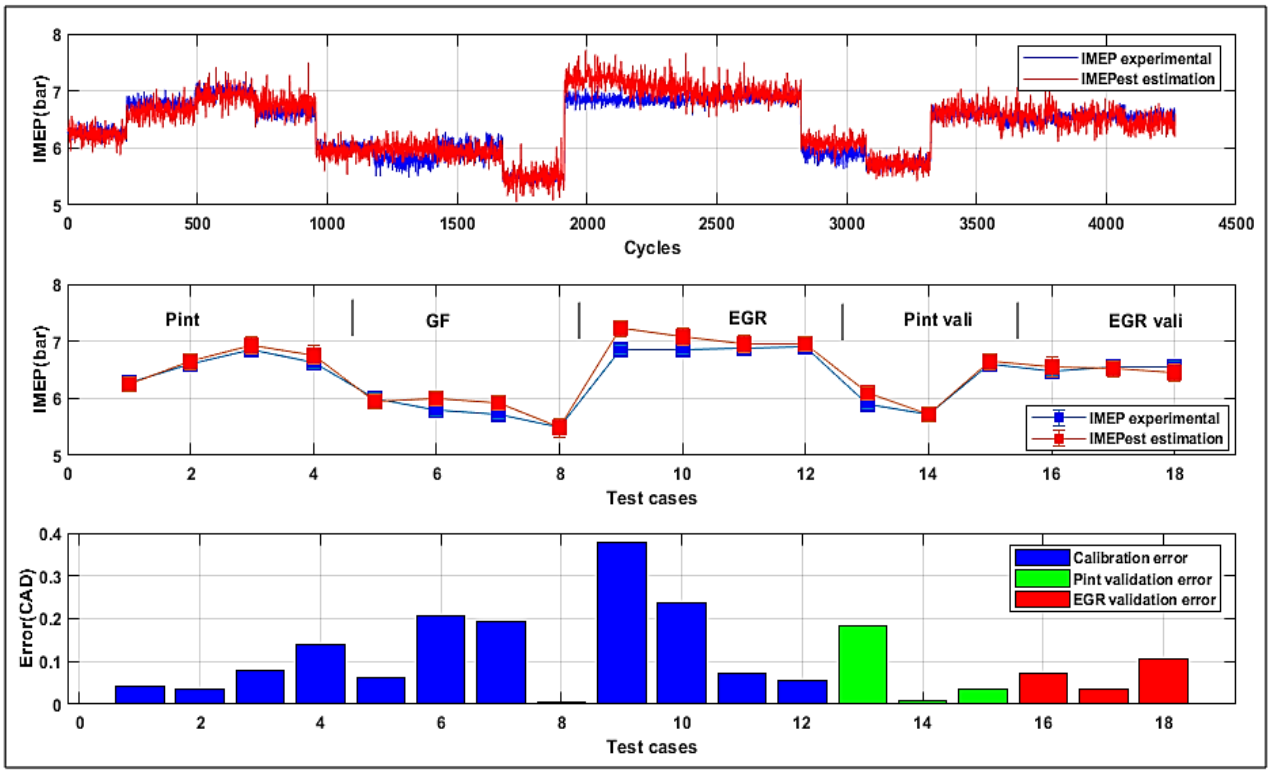

Figure 13 : IMEP estimation and validation, cycle to cycle IMEP, mean values and error bars

6.5. Transient condition validation

Transient condition data that was shown in Figure 5, has been used to test constants those obtained from calibration stage, on a transient condition of this type of engine. After applying the constants and comparing with experimental data, results were illustrated in Figure 14.

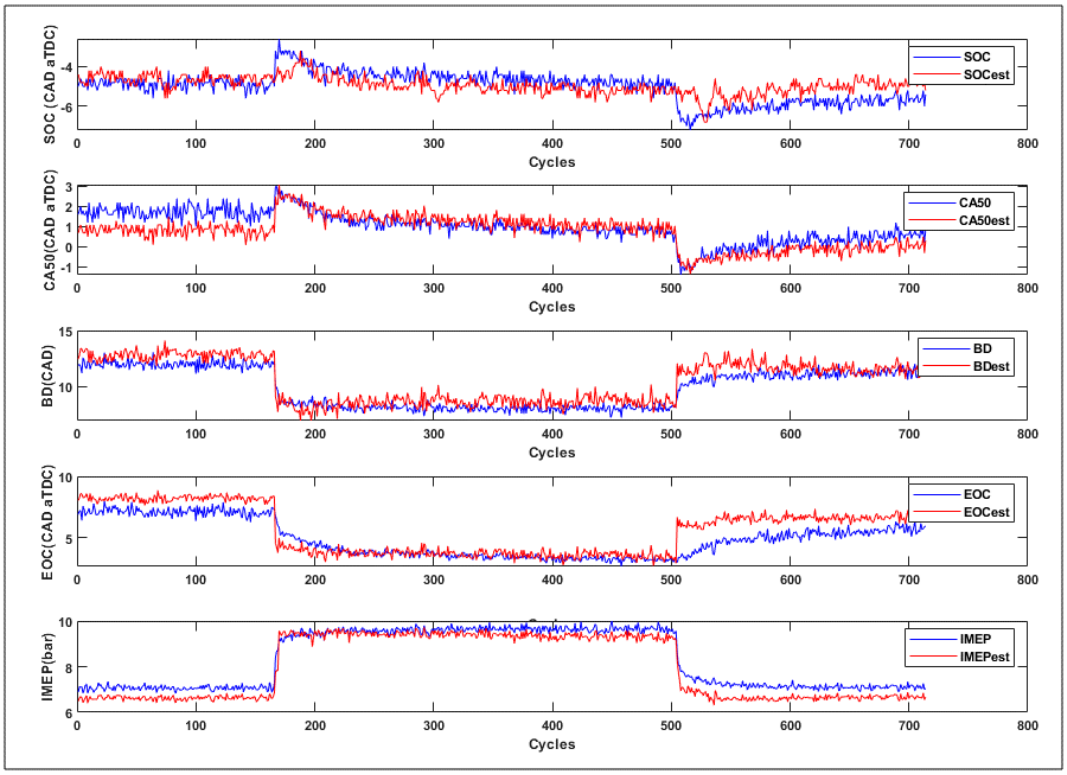

Figure 14: Transient condition validation and experimental comparison

SOC, CA50, BD, EOC and IMEP estimation were depicted in Figure 14. It is clear from this figure that there is a good trend in estimation of these engine characteristics. Maximum mean error for SOC estimation is 1.4 CAD and it is 0.6 CAD for estimation of CA50. BD and EOC have maximum mean error of 1.8 and 1.7 CAD, respectively. Estimation of IMEP has 0.8 bar maximum mean error which is in the same direction of experimental data Also there is maximum mean error of 0.8bar in IMEP estimation, according to figure 15 majority of data points in estimation errors have values under 0.4 bar which is under four percent error. According to IMEP estimation, equation 40, having good accuracy in estimation of SOC, BD and EOC cause to have better results for IMEP estimation.

Figure 15 shows data distribution accuracy in transient validation for various characteristic of engines. Most of the data in this condition test have acceptable error which is approximately below 2 units in each engine characteristic.

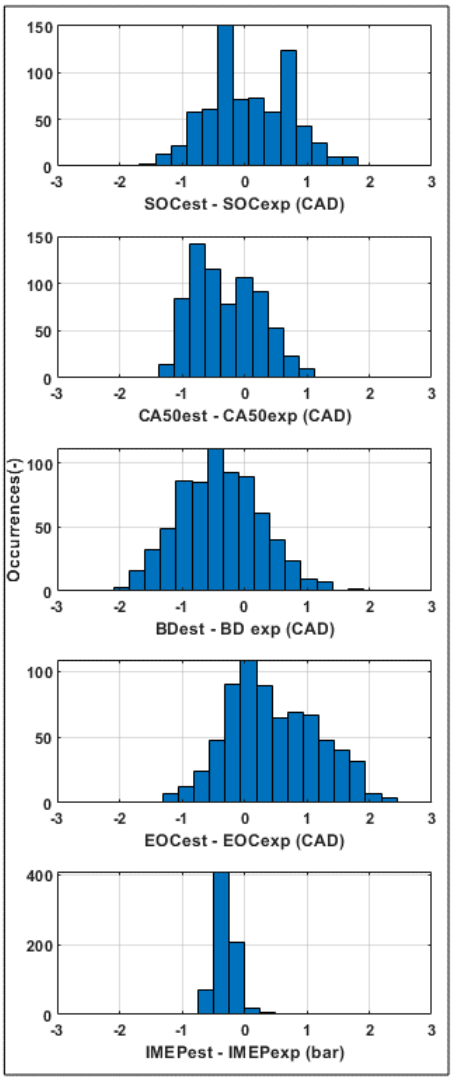

Figure 15: Data occurrences in transient case study validation

7. Conclusion

A COM solution was used for estimation of an RCCI Diesel/Gasoline six-cylinder CI engine. SOC, CA50 and BD are three combustion properties which were estimated from calibration and validation using five experimental datasets. According to figures 5 to 11, estimation results are with a good accuracy where the maximum mean error is about 1.9 CAD for BD. Other errors are less than 1 CAD, maximum error for SOC estimation is 1.7 CAD and it is 2.3 CAD for estimation of CA50. As a result of good accuracy in estimation and modeling of combustion process.

There is good trend in estimation of SOC, BD and CA50 despite of a small mean error in them. In EGR calibration and validation it seems that modeling could not capture the same accuracy for SOC estimation

but the error of this section is less than 2.3 CAD. It can be concluded that SOC estimation was affected by heating values of fuel mixture (gasoline and diesel) in comparison with EGR, so the effects of EGR changing could not make an impressive effect on the calibration process., As a result the trend of estimation and mean error in SOC estimation is slightly higher than that of other points. In CA50 and BD calibration estimation shows better results in GF below 0.5. It seems that in-cylinder non-linearity causes this error as the model uses a polynomial linear equation for applying GF effects. According to nature of in-cylinder combustion and as it was described before combustion spontaneous front speed is an N-variable function that depends on various conditions, also with considering this fact that combustion start from random points in whole cylinder domain. as a result, defining time function (time between SOI to SOC) from cumulative density function of all variables provides more accurate combustion modeling and predicting.

IMEP estimation in steady state condition has mean error less than 0.45 bar with acceptable trends in estimated results, error contribution of this engine property also shows that majority of estimated IMEP have error below 0.5 bar. As a lateral conclusion it is clear that EGR variation has no effective role in IMEP and as a result on engine output power.

Transient validation has also good results and trends. In this case study maximum mean error for SOC, CA50, BD and EOC are 1.4, 0.6, 1.8 and 1.7 CAD, respectively. Estimation of IMEP in this section has maximum mean error of 0.8 bar. The good accuracy in IMEP estimation is due to having good results and calibration in combustion characteristic of the engine such as SOC, BD and EOC.

8. Acknowledgement

The authors acknowledge the support of Spanish Ministerio de Economia, Industria y Competitivad through project TRA2016-78717-R (AEI/FEDER, EU). Alvin Barbier participation was funded through grant ACIF/2018/141, Programa Operativo del Fondo Social Europeo (FSE) de la Comunitat Valenciana 2014-2020. Alireza Kakoee participation was funded through grants 43/3/298624 from Iran ministry of science, research and technology.

9. REFERENCES

[1] Pachiannan,T.,Zhong, W., Rajkumar,S., He, Z., Leng, X., Wang, Q.(2015). 'A literature review of fuel effects on performance and emission characteristics of low-temperature combustion strategies', Applied Energy, Volume 251, 113380, ISSN 0306-2619

[2] Kakoee, A., Gharehghani, A.(2019). 'Comparative study of hydrogen addition effects on the natural-gas/diesel and natural-gas/dimethyl-ether reactivity controlled compression ignition mode of operation', Energy Conversion and Management,Volume 196, Pages 92-104,ISSN 0196-8904.

[3] Kakoee, A., Bakhshan, Y., Motadayen, S., Gharehghani, A.(2018).'An improvement of a lean burning condition of natural gas/diesel RCCI engine with a pre-chamber by using hydrogen',Energy Conversion and Management,Volume 166, Pages 489-499,ISSN 0196-8904

[4] Benajes, J., Molina, S., García, A.(2014). 'Eduardo Belarte, Michel Vanvolsem,An investigation on RCCI combustion in a heavy duty diesel engine using in-cylinder blending of diesel and gasoline fuels, Applied Thermal Engineering', Volume 63, Issue 1, ,Pages 66-76,ISSN 1359-4311.

[5] Guardiola, C.,Pla, B., Bares, P., Barbier, A.(2018).'A combustion phasing control-oriented model applied to an RCCI engine'IFAC-PapersOnLine, Volume 51, Issue 31, Pages 119-124, ISSN 2405-8963,

[6] Kakoee, A., Bakhshan, Y., Gharehghani, A., Salahi, MM.(2019). comparative study of hydrogen addition on combustion and emission characteristics of a natural-gas/dimethyl-ether RCCI engine with pre-chamber, Energy,Volume 186, 115878,ISSN 0360-5442,

[7] Yao, M., Zheng, Z., Liu, H.(2009). 'Progress and recent trends in homogeneous charge compression ignition (HCCI) engines', Progress in Energy and Combustion Science, Volume 35, Issue 5, Pages 398-437, ISSN 0360-1285.

[8] Benajes, J., Molina, S., García, A., Monsalve-Serrano, J.(2015). Effects of direct injection timing and blending ratio on RCCI combustion with different low reactivity fuels, Energy Conversion and Management, Volume 99, Pages 193-209, ISSN 0196-8904.

[9] Wissink, ML., Lim, JH., Splitter, DA., Hanson, RM., Reitz, RD.(2012). 'Investigation of Injection Strategies to Improve High Efficiency RCCI Combustion with Diesel and Gasoline Direct Injection'. ASME. Internal Combustion Engine Division Fall Technical Conference, 327-338.

[10] Carlucci, A.P., Laforgia, D., Motz, S., Saracino, R., Wenzel, S.P.(2014). 'Advanced closed loop combustion control of a LTC diesel engine based on in-cylinder pressure signals', Energy Conversion and Management, Volume 77, Pages 193-207,ISSN 0196-8904.

[11] Olsson, J., Tunestål, P., and Johansson, B. (2001). 'Closed-Loop Control of an HCCI Engine.' SAE Transactions 110: 1076-085.

[12] Hanson, R., and Reitz, R. (2013). 'Transient RCCI Operation in a Light-Duty Multi-Cylinder Engine.' SAE International Journal of Engines 6, no. 3: 1694-705.

[13] Arora, J.K. and Shahbakhti, M. (2017). 'Real-Time Closed-Loop Control of a Light-Duty RCCI Engine During Transient Operation'. SAE Technical Paper.2017

[14] Ravi, N., Roelle, M. J., Liao, H., Jungkunz, F., Chang, C., Park, S., Gerdes, J. C. (2010). 'Model-based control of HCCI engines using exhaust recompression'. IEEE Transactions on Control Systems Technology, 18(6), 1289-1302,

[15] Bekdemir, C., Baert, R., Willems, F., Somers, B.(2015). 'Towards Control-Oriented Modeling of Natural Gas-Diesel RCCI combustion'. SAE Technical Paper 2015-01-1745.

[16] Khodadadi Sadabadi, K. and Shahbakhti, M. (2016). 'Dynamic Modeling and Controller Design of Combustion Phasing for an RCCI Engin'. ASME, Dynamic Systems and Control Conference,

[17] Kondipati, NNT., Arora, JK., Bidarvatan, M., Shahbakhti, M.(2017). 'Modeling Design and Implementation of a Closed-Loop Combustion Controller for an RCCI Engine'. 4747-4752.

[18] Shahbakhti, M., and Koch, C. R.,(2007). 'Control Oriented Modeling of Combustion Phasing for an HCCI Engine,' American Control Conference, New York, NY, pp. 3694-3699.

[19] Livengood, J.C. and Wu, P.C.(1955). 'Correlation of auto ignition phenomena in internal combustion engines and rapid compression machines'. Symposium (International) on Combustion, 5(1), 347-356.1955.

[20] Khodadadi Sadabadi, K., Shahbakhti, M., Bharath,A., and Reitz, R.(2016). 'Modeling of Combustion Phasing of a Reactivity-Controlled Compression Ignition Engine for Control Applications.' International Journal of Engine Research 17, no. 4: 421–35.

[21] Sui, W., Pulpeiro González, J., Hall, CM.(2018). 'Modeling and Control of Combustion Phasing in Dual-Fuel Compression Ignition Engines'. ASME. J. Eng. Gas Turbines Power.;141(5):051005-051005-12.

[22] Shaver, G.M.; Gerdes, J.C.; Roelle, M.(2004). 'Physics-based closed-loop control of phasing, peak pressure and work output in HCCI engines utilizing variable valve actuation'. Proceedings of the American Control Conference, Boston, MA, USA, , pp. 150-155 vol.1.

[23] Mayhew, C. G., Knierim, K. L., Chaturvedi, N. A., Park, S., Ahmed, J., Kojic, A. (2009). 'Reduced-order modeling for studying and controlling misfire in four-stroke HCCI engines'. Proceedings of the 48h IEEE Conference on Decision and Control (CDC) held jointly with 2009 28th Chinese Control Conference, Shanghai, pp. 5194-5199.

[24] Chiang, C.J. and Stefano Poulou, A.G. (2006). 'Sensitivity analysis of combustion timing and duration of homogeneous charge compression ignition (HCCI) engines'. American Control Conference, Minneapolis, MN, pp. 6 pp.

[25] He, X., Donovan, M.T., Zigler, B.T., Palmer, T.R., Walton, S.M., Wooldridge, M.S., Atreya, A.,(2005). 'An experimental and modeling study of iso-octane ignition delay times under homogeneous charge compression ignition conditions', Combustion and Flame,Volume 142, Issue 3, Pages 266-275,ISSN 0010-2180

[26] Widd, A., Tunestal, P. and Johansson, R. (2008).'Physical Modeling and Control of Homogeneous Charge Compression Ignition (HCCI) engines,' 2008 47th IEEE Conference on Decision and Control, Cancun, pp. 5615-5620.

[27] Scott Goldsborough, S., (2009). 'A chemical kinetically based ignition delay correlation for iso-octane covering a wide range of conditions including the NTC region' ,Combustion and Flame,Volume 156, Issue 6, Pages 1248-1262,ISSN 0010-2180

[28] Kokjohn, S., Hanson, R., Splitter, D., & Reitz, R. (2010). Experiments and Modeling of Dual-Fuel HCCI and PCCI Combustion Using In-Cylinder Fuel Blending. SAE International Journal of Engines, 2(2), 24-39.

[29] Desantes, JM., Benajes, J., García, A., Monsalve-Serrano, J. (2014). 'The role of the in-cylinder gas temperature and oxygen concentration over low load reactivity controlled compression ignition combustion efficiency', Energy, Volume 78, Pages 854-868, ISSN 0360-5442.

[30] Benajes, J., Molina, S., Paster, J., Monsalve-Serrano, J.(2016). 'Effects of piston bowl geometry on Reactivity Controlled Compression Ignition heat transfer and combustion losses at different engine loads', Energy, Volume 98, Pages 64-77, ISSN 0360-5442

[31] Wu, Y., Hanson, R., Reitz, RD.(2014). 'Investigation of Combustion Phasing Control Strategy During Reactivity Controlled Compression Ignition (RCCI) Multi-cylinder Engine Load Transitions'. ASME. J. Eng. Gas Turbines Power.;136(9):091511-091511-10.

[32] Chen, JH., Hawkes, ER., Sankaran, R., Mason, SD., Hong, GL. (2006). 'Direct numerical simulation of ignition front propagation in a constant volume with temperature in homogeneities: I. Fundamental analysis and diagnostics', Combustion and Flame, Volume 145, Issues 1–2, Pages 128-144, ISSN 0010-2180.

[33] Karagiorgis, S., Collings, N., Glover, K., Coghlan, N., and Petridis, A.(2006). 'Residual Gas Fraction Measurement and Estimation on a Homogeneous Charge Compression Ignition Engine Utilizing the Negative Valve Overlap Strategy'. SAE Paper No. 2006-01-3276.

[34] Raut, A., Irdmousa, B.K., Shahbakhti, M.(2018). 'Dynamic modeling and model predictive control of an RCCI engine', Control Engineering Practice, Volume 81, Pages 129-144, ISSN 0967-0661,

[35] Cavina, N., Siviero, C., and Suglia. C. (2004). 'Residual Gas Fraction Estimation: Application to a GDI Engine with Variable Valve Timing and EGR'. SAE, Paper No. 2004-01-2943.

[36] Heywood, J. B. (1988). Internal combustion engine fundamentals. Mcgraw-Hill New York.

[37] Bidarvatan, M., Shahbakhti, M., Jazayeri, S.A., Koch, C.R.(2014). 'Cycle-to-cycle modeling and sliding mode control of blended-fuel HCCI engine', Control Engineering Practice, Volume 24, Pages 79-91, ISSN 0967-0661.

[38] Raut, A., Bidarvatan, M., Borhany, H., and Shahbakhti, M.(2018). 'Model Predictive Control of an RCCI Engine', 2018 Annual American Control Conference (ACC), June 27–29,. Wisconsin Center, Milwaukee, USA

[39] Bengtsson, J. , Strandh, P. , Johansson, R. , Tunestål, P. and Johansson, B. (2004). 'Closed-loop combustion control of homogeneous charge compression ignition (HCCI) engine dynamics'. Int. J. Adapt. Control Signal Process.

[40] Taghavi, M., Gharehghani, A., Bakhtiari Nejad, F., Mirsalim, M.(2019). 'Developing a model to predict the start of combustion in HCCI engine using ANN-GA approach, Energy Conversion and Management, Volume 195,2019,Pages 57-69,ISSN 0196-8904